XLI CILAMCE
XLI Ibero-Latin American Congress on Computational Methods in Engineering
16-19 November, 2020 FOZ DO IGUAÇU PARANÁ - BRAZIL

Effect of lateral movement type on earth pressures developed behind the abutment of a semi-integral bridge

Pedro H. dos S. Silva[1], Yuri D. J. Costa[1], Jorge G. Zornberg[2], Carina M. L. Costa[1]

[1]*Department of Civil Engineering, Federal University of Rio Grande do Norte*
University Campus, 59072-970, Rio Grande do Norte, Brazil
eng.phsilva@outlook.com, ydjcosta@ct.ufrn.br, carina@ct.ufrn.br
[2]*Department of Civil, Architectural and Environmental Engineering, The University of Texas at Austin*
301 E. Dean Keeton St., 78712, Texas, United States of American
zornberg@mail.utexas.edu

Abstract. Semi-integral abutment bridges are constructed without thermal expansion joints, and the superstructure-abutment system is not integrally connected to the substructure. In view of this peculiar characteristic, the abutment undergoes combined movements of translation and rotation due to the expansion and contraction of the superstructure. This work proposes to analyze the effect of different lateral movements on the earth pressures developed behind the abutment of a semi-integral bridge. Numerical simulations were carried out by using a finite element model. Lateral movements of the abutment were simulated in three different conditions: combined rotation and translation (Case 1), rotation only (Case 2), and translation only (Case 3). Predicted lateral earth pressures were compared with experimental field data obtained from a semi-integral bridge abutment. Predicted values were obtained at the same position where the field measurements were performed on the abutment. The best match between field and numerical pressures were obtained with Case 1. During expansion phases of the bridge superstructure, Case 2 slightly underestimated the lateral earth pressures, while Case 3 overestimated them. The opposite occurred during contraction phases. The combined movement of rotation and translation proved to be more suitable to represent the lateral movements of the bridge abutment in field conditions.

Keywords: integral bridge, finite element, abutment, lateral earth pressure.

1 Introduction

According to Husain and Bagnariol [1], semi-integral abutment bridges (SIABs) are structural systems built without thermal expansion joints, but with bearing pads, at the abutments. In these structural systems, the abutment and the superstructure of the bridge are integrally connected, forming a continuous system without connection with the substructure of the bridge. Maruri and Petro [2] affirm that the main advantage of using SIABs is the reduction of construction and maintenance costs related to the absence of thermal expansion joints since these devices require adequate and frequent maintenance due to their low durability compared to other bridge components. For Mistry [3], the absence of thermal expansion joints reduces the bridge susceptibility to problems regarding improperly functioning joints due to corrosion that allows attacks of chemical agents on other bridge elements.

Because of the peculiar characteristic of SIABs, Ng et al. [4] state that expansion and contraction horizontal movements of the bridge superstructure, caused by temperature variations, are integrally transferred to the bridge abutment, resulting in lateral movements. ABNT NBR 7187:2003 [5] suggests that the temperature variation in the bridge should be considered as indicated in section 11 of ABNT NBR 6118:2003 [6]. ABNT NBR 6118:2014 [7], which replaced ABNT NBR 6118:2003 [6], recommends considering a uniform temperature distribution in the bridge structure, which can result in a translation movement of the abutment. ABNT NBR 6118:2014 [7] also recommends adopting a linear temperature distribution in the bridge structure for the cases of non-uniform temperature distributions. In this case, the abutment can undergo rotation or a combined movement of rotation and

translation.

Fartaria [8] carried out numerical simulations, using the finite element method, of an integral bridge abutment upon three different movements of the abutment: rotation, translation, and combined movement involving translation and rotation. The abutment, modeled as a plate element, has a height of 4 m and is embedded in a sandy soil, which was modeled by using the constitutive model that uses the Mohr-Coulomb failure criterion. The results showed that the translation movement of the abutment presented the largest lateral earth pressures, while the rotation movement showed the lowest lateral earth pressures. The combined movement of translation and rotation presented intermediate values of lateral earth pressure.

The type of lateral movement the bridge abutment experience can result in different lateral earth pressure distributions on the abutment. The lateral movements depend on the temperature distribution along the height of the bridge superstructure, which cannot simply be assumed to be uniform. Understanding the lateral earth pressures' response upon different forms of lateral movements of the bridge abutment contributes to achieving more accurate predictions of field conditions from numerical modelling. In view of this, the present paper analyzes the impact of the form of lateral movement of a bridge abutment on the earth pressures developed behind the abutment of a semi-integral bridge.

2 Methodology

Numerical simulations of a semi-integral bridge abutment were carried out using the software Plaxis 2D 2016, which uses the finite element method (FEM). Plane-strain conditions were used in a two-dimensional finite element analysis. A numerical model was developed and calibrated based on the field data from the west abutment of a semi-integral abutment bridge instrumented and monitored by Walter [9]. The model boundaries extended to a width of 40 m in the horizontal direction and a depth of 20 m in the vertical direction. These dimensions were chosen based on the information of Knappett et al. [10] and Rawat and Gupta [11] and were assumed to be enough to exclude boundary effects. Vertical boundaries were fixed in x-direction and free in y-direction. The bottom boundary was fixed in both directions, while the top boundary was free in both directions. The abutment-cap system was assumed as a reinforced concrete structure supported by a driven steel sheet pile foundation. According to Walter [9], the site subsoil at the west abutment can be categorized by a silty sand layer over a sandy clay layer with gravel spaced at 1V:3H (where V is vertical, and H is horizontal) increments along the width of the abutment. Therefore, a 6.5-m silty sand layer over a 13.5-m sandy clay layer and gravel spaced at 1V:3H increments next to the abutment were adopted in the numerical model. The thickness of the soil layers was chosen based on information provided by Zornberg et al. [12]. The finite element mesh used in the numerical simulations was a very fine mesh composed of 15-node triangular elements and with automatic refinement on the interfaces of the soil-structure interaction. Figure 1 shows the dimensions adopted to the abutment-cap system and the finite element mesh used in the numerical simulations.

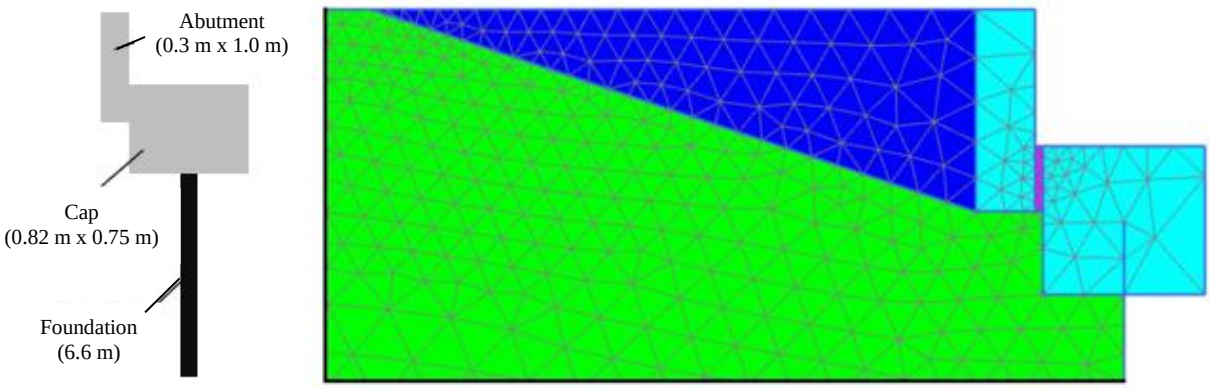

Figure 1. Abutment-cap system (left) and finite element mesh (right).

The behavior of the soil materials was represented by the Hardening Soil hyperbolic constitutive model. According to Khanal [13], this constitutive model is based on the Plasticity Theory and was developed to simulate

sandy and clayey soils. The structural concrete and the fiberboard were modeled with the linear elastic constitutive model. The sheet piles of the foundation were modeled using plate elements and the behavior was assumed as linear elastic. Soil-structure interaction was taken into consideration in the model by using interface elements with strength reduction factors (R_{inter}) equal to 0.5 for the soil-steel interface and 0.7 for the soil-concrete interface. The R_{inter} values were chosen based on the suggestions made by Naval Facilities Engineering Command [14], Brinkgreve et al. [15], and Muszynski and Wyjadlowski [16]. A virtual thickness factor of 0.1 was applied to the interface boundaries.

The parameters of the clayey soil adopted to the numerical model were unsaturated unit weight (γ_{unsat}) equal to 19 kN/m³, saturated unit weight (γ_{sat}) equal to 22 kN/m³, secant stiffness modulus at 50% of the peak load (E_{50}) equal to 60 MPa and undrained shear strength (S_u) equal to 210 kPa. The parameters adopted for the sandy soil were γ_{unsat} equal to 17 kN/m³, γ_{sat} equal to 20 kN/m³, E_{50} equal to 40 MPa, effective cohesion (c') equal to 15 kPa and effective internal friction angle (ø') equal to 31.5°. The parameters adopted for the gravel were γ_{unsat} equal to 20 kN/m³, γ_{sat} equal to 23 kN/m³, E_{50} equal to 32 MPa, c' equal to 1 kPa and ø' equal to 40°. These soil parameters were estimated based on values for typical soil types proposed by Poulos and Davies [17], Stroud and Butler [18], Mesri [19], Kulhawy and Mayne [20], and Tomlinson [21], considering the soil characteristics presented by Zornber et al. [12]. The parameters for the concrete adopted in the numerical model were unit weight (γ) equal to 25 kN/m³, Young's modulus (E) equal to 30 GPa and Poisson's ratio (ν) equal to 0.2. Parameters used for the steel sheet piles were weight (w) equal to 1.182 kN/m/m, normal stiffness (EA) equal to 3.163 x 10^6 kN/m, flexural rigidity (EI) equal to 73.27 x 10^3 kN·m²/m and ν equal to 0.3. The structural parameters were estimated based on information from AASHTO [22] and Gerdau [23]. Further details about the numerical model can be found in Zornberg et al. [12].

Three different lateral movement types of the abutment were simulated by applying 100 cycles of prescribed horizontal displacements, as to represent the cyclic lateral displacements of the abutment due to daily maximum expansions and contractions of the bridge. The first movement type (Case 1) included applying the displacement at the top of the abutment, resulting in a combined movement of rotation and translation. In the following movement type (Case 2), the displacement was linearly imposed along the abutment height. The displacement was equal to zero at the abutment base and maximum at the abutment top, resulting in rotation of the abutment. The last movement type (Case 3) consisted of applying the displacement uniformly along the abutment height, resulting in a translation movement. Figure 2 presents the three simulated lateral displacement types.

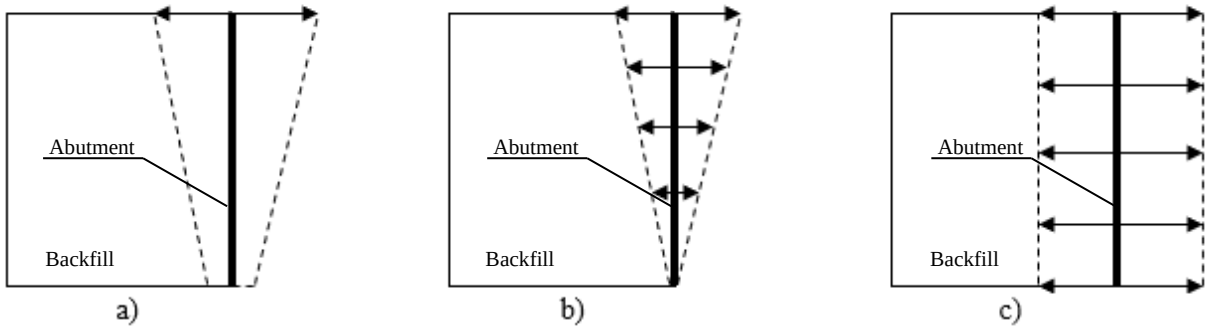

Figure 2. Simulated lateral displacement types: a) Case 1 (rotation + translation); b) Case 2 (rotation); c) Case 3 (translation).

The lateral displacements (δ_h) at the abutment were estimated by Eq. 1, as suggested by Karalar and Dicleli [24] and Murphy and Yarnold [25]:

$$\delta_h = \frac{\alpha L \Delta T}{2} \tag{1}$$

where α is the coefficient of thermal expansion, L is the length and ΔT is the temperature variation. The α value assumed for the concrete was 10.8 x 10^{-6}/°C and is in the range recommended by AASHTO [22] in the absence of laboratory tests or more precise data. The ΔT and L values were obtained from Walter [9]. Figure 3 shows the estimated values of prescribed horizontal displacements considering the first 100 days of monitoring.

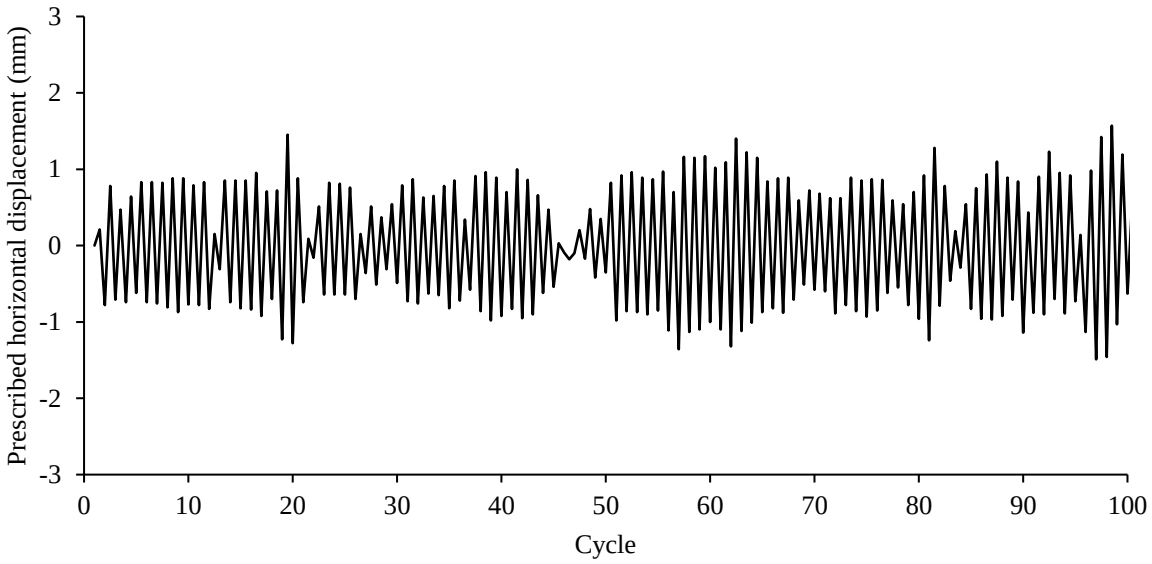

Figure 3. Estimated prescribed displacement representing the lateral movements of the abutment.

The lateral earth pressures, predicted by the numerical model, for the three analyzed movements were compared with the field data (Case 0). The predicted values of lateral earth pressures were obtained at the same position where the field measurements were collected in the abutment (the bottom third of the abutment).

3 Results and discussion

Figures 4 and 5 show the comparison between the lateral earth pressures at the end of daily cycles of expansion and contraction of the bridge for the analyzed cases, respectively.

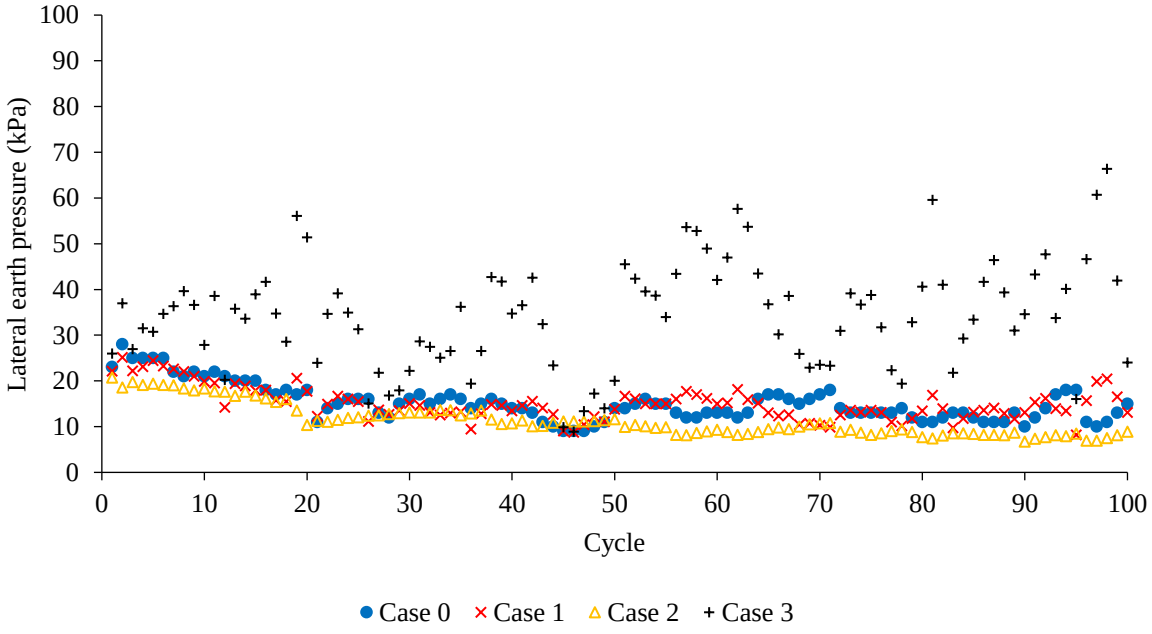

Figure 4. Lateral earth pressures at the end of daily cycles: bridge expansion.

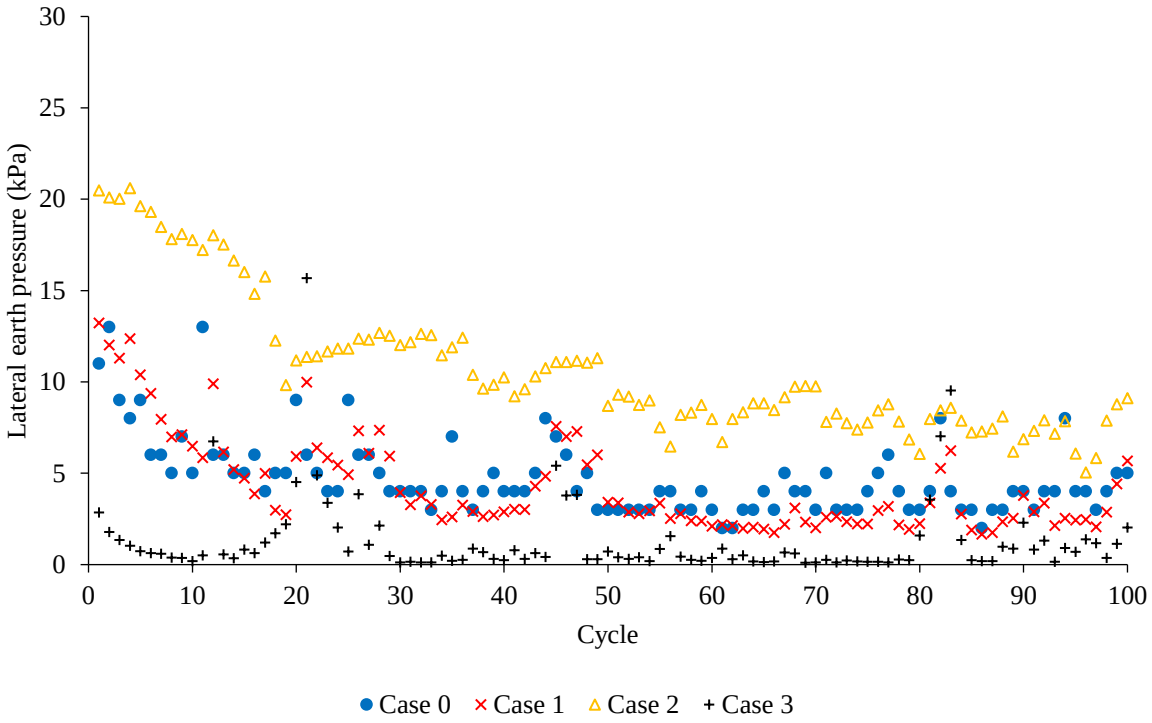

Figure 5. Lateral earth pressures at the end of daily cycles: bridge contraction.

The results showed that the best match between field and numerical pressures was obtained with Case 1 for both expansion and contraction of the bridge superstructure. During expansion phases of the bridge superstructure, Case 2 slightly underestimated the lateral earth pressures while Case 3 overestimated them. During bridge contraction, Case 2 overpredicted the pressures, while Case 1 underpredicted them. Moreover, the lateral earth pressures were virtually the same for the expansion and contraction phases of the bridge superstructure in Case 2. The combined movement of rotation and translation proved to be more suitable to represent the lateral movements of the bridge abutment in the field.

The results can be related to the lateral movement type of the bridge abutment. According to Lee [26], the temperature along the height of the bridge superstructure presents a non-linear distribution, which results in a combined movement of translation and rotation of the bridge abutment, as reported by Ng et al. [4]. This can explain the best match between field and numerical pressures obtained with Case 1. In Case 2, the rotation caused the smallest lateral displacements of the bridge abutment where the measurements were obtained in field (bottom third of the bridge abutment), as compared to Cases 1 and 3. In this case, the backfill was not significantly compressed and decompressed during the bridge expansion and contraction, respectively, which can explain the lateral earth pressures obtained in Case 2. Finally, Case 3 presented the largest values of lateral displacements at the bottom third of the bridge abutment, which can explain the overestimated predicted earth pressures for the bridge expansion and the underestimated predicted earth pressures for the bridge contraction.

4 Concluding remarks

The present study analyzed the effect of different lateral movements on the earth pressures developed behind the abutment of a semi-integral bridge. Numerical simulations were carried out by using a finite element model proposed to a semi-integral bridge abutment. Lateral movements of the abutment were simulated in three different conditions: combined rotation and translation (Case 1), rotation only (Case 2), and translation only (Case 3). The main findings of this work are as follows:

- The best match between field and numerical pressures were obtained with rotation and translation of the bridge abutment.

- During expansion phases of the bridge superstructure, displacements involving abutment rotation only slightly underestimated the lateral earth pressures, while displacements involving abutment translation only gave overestimated results. The opposite occurred during bridge contraction phases.
- The combined movement of rotation and translation showed to be more suitable to represent the lateral movements of the bridge abutment in field conditions.

Authorship statement. The authors hereby confirm that they are the sole liable persons responsible for the authorship of this work, and that all material that has been herein included as part of the present paper is either the property (and authorship) of the authors, or has the permission of the owners to be included here.

References

[1] I. Husain and D. Bagnariol. *Semi-integral abutment bridges*. Ministry of Transportation, 1999.
[2] R. F. Maruri and S. H. Petro. Integral abutments and jointless bridges (IAJB) 2004 survey summary. In: *The 2005 – FHWA Conference*, pp. 12–29, 2005.
[3] V. C. Mistry. Integral abutment and Jointless bridges. In: *The 2005 – FHWA Conference*, pp. 3–11, 2005.
[4] C. W. W. Ng, S. M. Springman and A. R. M. Norrish. Centrifuge modeling of spread-base integral bridge abutments. *Journal of Geotechnical and Geoenvironmental Engineering*, vol. 124, n. 5, pp. 376-388, 1998.
[5] ABNT. *ABNT NBR 7183:2003: projeto de pontes de concreto armado e de concreto protendido – procedimento*. ABNT, 2003.
[6] ABNT. *ABNT NBR 6118:2003: projeto de estruturas de concreto – procedimento*. ABNT, 2003.
[7] ABNT. *ABNT NBR 6118:2014: projeto de estruturas de concreto – procedimento*. ABNT, 2014.
[8] C. I. P. Fartaria. *A interação estutura-solo em pontes integrais*. Master Thesis, Universidade Técnica de Lisboa, 2012.
[9] J. R. Walter. *Experimental and numerical investigation of integral/semi-integral bridge abutments for Texas conditions*. Master Thesis, The University of Texas at Austin, 2018.
[10] J. A. Knappett, K. Caucis, M. J. Brown, J. R. Jeffrey and J. D. Ball. CHD pile performance: part II – numerical modelling. *Proceedings of the Institution of Civil Engineers – Geotechnical Engineering*, vol. 169, n. 5, pp. 436–454, 2016.
[11] S. Rawat and A. S. Gupta. Numerical modelling of pullout of helical soil nail. *Journal of Rock Mechanics and Geotechnical Engineering*, vol. 9, n. 4, pp. 648–658, 2017.
[12] J. G. Zornberg, B. Mofarraj, Y. Costa, P. Silva and T. Helwig. *TxDOT project 0-6936: development of integral/semi-integral abutments for Texas bridges*. The University of Texas at Austin, 2019.
[13] S. Khanal. *Backcalculation of plate loading tests using Plaxis 2D and the hardening soil model*. Master Thesis, Norwegian University of Science and Technology, 2013.
[14] Naval Facilities Engineering Command. *Foundation and earth structures*. Naval Facilities Engineering Command, 1986.
[15] R. B. J. Brinkgreve, E. Engin and W. M. Swolfs. *Plaxis 2D version 2012 manual*. Balkema, 2012.
[16] Z. Muszynski and M. Wyjadlowski. Assessment of the shear strength of pile-to-soil interfaces based on pile surface topography using laser scanning. *Sensors*, vol. 19, n. 5, pp. 1-21, 2019.
[17] H. G. Poulos and E. H. Davies. *Elastic solutions for soil and rock mechanics*. John Williams & Sons, 1974.
[18] M. A. Stroud and F. G. Butler. The standard penetration test and the engineering properties of glacial materials. In: *Symp. on Engineering Properties of Glacial Materials*, pp.117-128, 1975.
[19] G. Mesri. New design procedure for stability of soft clays. *J. Geotech. Eng. Div.*, vol. 101, pp. 409-412, 1975.
[20] F. H. Kulhawy and P. W. Mayne. *Manual on estimating soil properties for foundation design*. Cornell University, 1982.
[21] M. J. Tomlinson. *Pile design and construction practice*. E & FN Spon, 1993.
[22] AASHTO. *LRFD bridge: design specifications*. AASHTO, 2012.
[23] Gerdau. *Steel sheet piling: quick reference guide*. Gerdau, 2019.
[24] M. Karalar and M. Dicleli. Fatigue in jointless bridge H-piles under axial load and thermal movements. *Journal of Constructional Steel Research*, vol. 147, pp. 504-522, 2018.
[25] B. Murphy and M. Yarnold. Temperature-driven structural identification of a steel girder bridge with an integral abutment. *Engineering Structures*, vol. 115, pp. 209-221, 2018.
[26] D. J. Lee. *Bridge bearings and expansion joints*. E & FN Spon, 1994.